NIH Public Access
Author Manuscript
JACC Cardiovasc Imaging. Author manuscript; available in PMC 2010 November 1.

Published in final edited form as:
JACC Cardiovasc Imaging. 2009 November ; 2(11): 1321–1331. doi:10.1016/j.jcmg.2009.09.002.

Interventional Cardiovascular Magnetic Resonance Imaging:

A New Opportunity for Image-Guided Interventions

Christina E. Saikus, BS and **Robert J. Lederman, MD**
Translational Medicine Branch, Division of Intramural Research, National Heart, Lung, and Blood Institute, National Institutes of Health, Bethesda, Maryland

Abstract

Cardiovascular magnetic resonance (CMR) combines excellent soft-tissue contrast, multiplanar views, and dynamic imaging of cardiac function without ionizing radiation exposure. Interventional cardiovascular magnetic resonance (iCMR) leverages these features to enhance conventional interventional procedures or to enable novel ones. Although still awaiting clinical deployment, this young field has tremendous potential. We survey promising clinical applications for iCMR. Next, we discuss the technologies that allow CMR-guided interventions and, finally, what still needs to be done to bring them to the clinic.

Keywords

iCMR; CMR; MRI; image-guided interventions; endovascular; structural heart disease; electrophysiology; pediatrics

Minimally invasive and catheter-based therapies are targeting increasingly complex pathologies. This agenda requires better procedural image guidance (Table 1). Interventional cardiovascular magnetic resonance (iCMR) proposes to use the superb tissue imaging afforded by cardiovascular magnetic resonance (CMR) as a surrogate for direct surgical visualization. By providing multiple views and real-time functional imaging without ionizing radiation exposure, CMR could guide traditional interventional procedures and enable novel ones. We provide a brief overview of cardiovascular procedures that could benefit from real-time CMR guidance, followed by technical advances helping to move toward clinical testing.

Clinical Targets

Catheter-based endovascular interventions

CMR visualizes vessel wall and lumen without exogenous contrast. Interest in atherosclerosis imaging fueled much of the early work in intravascular CMR. Building on internal receiver coils for high-resolution intracardiac ^{31}P nuclear magnetic resonance (1), local endovascular coils were developed to characterize arterial wall composition with improved signal-to-noise ratio and resolution (2,3). Flow and motion, however, remain significant challenges to high-resolution magnetic resonance (MR) vessel images with realistic scan times in vivo.

Vascular interventions such as angioplasty and stenting under CMR could reduce radiation and iodinated contrast exposure compared with X-ray procedures. The use of CMR may also allow

Reprint requests and correspondence: Dr. Robert J. Lederman, Translational Medicine Branch, Division of Intramural Research, National Heart, Lung, and Blood Institute, National Institutes of Health, Building 10, Room 2c713, MSC1538, Bethesda, Maryland 20892-1538. ledermar@nhlbi.nih.gov.

NIH-PA Author Manuscript
NIH-PA Author Manuscript
NIH-PA Author Manuscript

NIH-PA Author Manuscript

NIH-PA Author Manuscript

NIH-PA Author Manuscript

image-based monitoring for serious complications such as vessel wall dissection or perforation (4,5). Newer stent alloys (including Nitinol and nickel-cobalt-chromium) are more compatible with CMR than older stainless-steel materials. Despite a dearth of other commercial devices suitable for interventional CMR, numerous endovascular procedures have been demonstrated in pre-clinical and early clinical studies. Although coronary catheterization and stenting have been performed under CMR guidance in healthy animals (6–8), we caution that clinical CMR lacks sufficient spatial or temporal resolution to guide meaningful clinical coronary interventional procedures.

Larger peripheral vessels such as aorta and iliac arteries are more attractive targets for CMR-guided procedures. Simple iliac angioplasty and stenting was performed in human feasibility studies by Manke et al. (9), albeit with limited imaging guidance. Renal artery stenting has been conducted solely under CMR in an animal renal artery stenosis (10). CMR-directed tube endografts repaired porcine abdominal aortic aneurysms (11) and thoracic aortic dissection after distinguishing true and false lumens (12). Aortic coarctation stenting with CMR guidance also has been explored (5). The authors of a clinical pilot study (13) successfully demonstrated CMR-assisted angioplasty for aortic coarctation in combination with X-ray.

Completely blocked vessel segments (chronic total occlusions) are virtually invisible in X-ray angiography where contrast cannot enter the obstructed lumen. The use of CMR can help to depict the mural contour of the occluded vessel and can help avoid perforation. Recanalization of an animal model carotid chronic total occlusion with the use of a custom active CMR device was significantly more successful than X-ray-guided alternatives (14). Newer devices are being developed that clearly indicate the device position during recanalization (15).

Moving beyond the vessels: extra-anatomic bypass, structural heart, and biological therapies

The use of CMR could allow catheter-based procedures to escape the traditional confines of vascular lumens. Extra-anatomic bypass, directly connecting two otherwise-unconnected vascular structures, might be enabled without surgery because of CMR guidance. In transjugular intrahepatic portosystemic shunt procedures, CMR helped reduce the number of needle passes needed to connect the hepatic to portal vein within the liver (16). Mesocaval puncture is an alternative portocaval trajectory enabled by CMR and custom-designed needle devices (17). A nonsurgical Blalock-Taussig subclavian-pulmonary shunt is a tantalizing potential application of this technology.

Structural heart disease interventions may benefit from the use of CMR in visualizing critical anatomy. CMR has guided-needle (18) and laser (19) atrial septal puncture and delivery of Nitinol closure devices for atrial septal defects (20–22) in swine. The use of CMR has enhanced positioning (with regard to myocardial fibrous skeleton and coronary arteries) and monitoring of transcatheter (23) and surgical transapical (24) (Fig. 1) aortic valve implants in swine with immediate evaluation of valve performance and flow. Hybrid imaging guidance for valve placement is also under development with the use of an adjacent “CMR-friendly” X-ray fluoroscope at the edge of the magnet (25).

With the development of novel biologic treatments, including local small molecule, gene, or cellular agents, CMR could play an important role in testing, delivering, and monitoring these therapies. The use of CMR provides enhanced catheter-based endomyocardial targeting and interactive imaging of local cell or drug accumulation and dispersion compared with X-ray or electroanatomic imaging (26,27). Several groups (28–31) have demonstrated successful delivery or tracking of cell and gene products to myocardial targets in animals by using CMR.

NIH-PA Author Manuscript

NIH-PA Author Manuscript

NIH-PA Author Manuscript

Pediatrics

Pediatric patients stand to gain much from CMR-guided interventional procedures. Children with congenital heart disease often require multiple catheterizations to assess physiological parameters and for treatment that might avoid or delay open-heart surgery. Each interventional procedure, however, is offset by the risk for mechanical complications and possible long-term consequences from X-ray exposure. Children are especially susceptible to radiation injury, and pediatric interventions often are protracted, contributing further to the risk of chromosomal damage and malignancy (32). For medical staff, occupational X-ray exposure risks cancer and cataracts (33), whereas protective lead garments risk chronic orthopedic injury (34).

Razavi et al. (35) brought real-time CMR into the clinic. They guided diagnostic catheterizations and electrophysiological procedures in children and adults with congenital heart disease by using a combined MR/X-ray suite. The use of CMR-guided catheterization has also enhanced the assessment of total or split pulmonary vascular resistance in patients (36,37). Beyond invasive diagnostics, CMR might enhance treatment of structural pathology in children and adults with congenital heart disease. Interventions for structural abnormalities such as ventricular septal defect could benefit from improved visualization of the septal defect and close procedural monitoring. Pre-clinical CMR-guided pulmonary artery and valve stenting (38) suggests percutaneous pulmonary valve replacement (39) might be feasible under CMR. As mentioned previously, CMR may enable percutaneous creation and closure of pulmonary-systemic shunts.

Electrophysiology (EP)

Interventional CMR proposes one-stop visualization of cardiac surfaces being mapped, monitoring of ablation, and assessment of ablation lesions. Compared with ablation under direct surgical exposure, conventional catheter ablations of atrial fibrillation or ventricular-tachycardia are lengthy and complex, in part because of inadequate targeting and visualization of ablation lesions. The use of CMR offers value beyond creating baseline roadmaps now widely imported into electroanatomic mapping systems (40). Investigators have begun to correlate ablation lesions to successful rhythm therapy (41,42). MR-compatible cardiac monitoring and ablation systems have enabled simple CMR-guided EP procedures (4,43–45). Figure 2 displays a sample CMR-guided EP mapping and recording study (45). Recently, Nazarian et al. (46) at Johns Hopkins demonstrated the feasibility of real-time CMR-guided EP mapping in 2 patients.

Multimodality image guidance

X-ray combined with magnetic resonance imaging, referred to as coregistration or XFM (X-ray fused with magnetic resonance imaging), overlays previously acquired MR images to enhance otherwise-difficult X-ray fluoroscopy procedures. These XFM procedures can benefit from the wide armamentarium of X-ray-compatible catheter equipment, along with additional 3-dimensional (3D) information about target vascular structures afforded by previous CMR. This multimodality approach has been used clinically in complex X-ray procedures such as biopsy of the myocardial free wall (47). The use of XFM also enabled precise endomyocardial injections (48) and a complex repair of membranous ventricular septal defects with significantly decreased fluoroscopy times in animal studies (49). Clinical EP studies already combine CMR roadmaps in commercial electroanatomic mapping systems (40).

In XFM, 3D contours of cardiovascular structures from CMR are overlaid on live X-ray (Fig. 3). Views update as the C-arm or table position changes. X-ray and CMR can be coregistered by the use of a shared table space (50), but patient movement causes misregistration. External fiducial marker beads on the patient can align MR and X-ray acquisitions even after patients move (47,51). Static roadmaps also become inaccurate from respiratory and cardiac motion,

NIH-PA Author Manuscript

NIH-PA Author Manuscript

NIH-PA Author Manuscript

which can be corrected by the use of more sophisticated techniques (52). Catheter position can be computed from 2 X-ray projections and back-displayed on a 3D MR roadmap.

Interventional MRI in other clinical disciplines

Several other clinical disciplines have embraced interventional MRI to guide critical procedures. Most enjoy targets that are relatively accessible, immobile, or require short, straight-needle devices. Neurosurgeons routinely use pre-procedural MRI with stereotactic frames for biopsies and resections; many conduct intraoperative MRI to guide, for example, tumor resection margins (53) or placement of deep-brain stimulation electrodes (54). Biopsy is also conducted under MRI for suspected liver, breast, and prostate malignancies (55). Tumor cryo- and radiofrequency ablation benefit from MRI guidance, which creates real-time temperature maps of target tissue (56). The use of MRI enhances orthopedic biopsies, injections, and other therapies as well (57). Many of these applications have fueled development of local imaging coils and MR-compatible manipulators and robotics (58).

Technology Behind iCMR

In this section we review advances in scanner design, imaging, and catheter devices that enable iCMR. We also discuss the remaining hurdles to clinical use.

Interventional suite and scanner selection

Short, wide, closed-bore 1.5- and 3.0-T scanners are now available. These systems provide superior image quality than earlier lower-field open magnets. Wide-bore scanners also allow satisfactory trans-femoral access to patients for interventional procedures compared with earlier closed-bore machines. The use of 3.0-T offers the potential to increase resolution and signal-to-noise ratio, but 3.0-T has been challenging to use with workhorse imaging techniques considered essential at 1.5-T.

Most research sites colocalize or combine MRI and X-ray angiography equipment to allow combined procedures and angiographic bailout (Fig. 4). Transfer tables or mobile MRI units (59) permit elective intermodality transfer or emergency evacuation. In a properly shielded room, both systems also run independently as MRI scanner and X-ray interventional labs. Fiberoptic or pneumatic headset systems with noise cancellation allow staff and patients to communicate despite loud acoustic MRI noise.

Real-time CMR

Steady-state free precession (often referred to as TrueFISP, FIESTA, or FFE) provides excellent blood and myocardial contrast in electrocardiogram-gated (nonreal-time) acquisitions. Steady-state free precession is now widely available in real time and has become the “workhorse” pulse sequence for interventional procedures. That said, it is no simple feat to acquire, reconstruct via computer, and display CMR images in less than a quarter second. Newer parallel techniques that use large receiver coil arrays and advanced computational techniques (60–62) allow even-faster scanning. Coupled with high-performance computing multiple-processor systems, real-time CMR is now available with image updates at 10 frames/s. Other phenomena, such as blood flow and myocardial tags, also can be imaged in real time. Although these MR images have a relatively small pixel matrix compared with X-ray (192 × 128 vs. 1,024 × 1,024), they are comparably rich in information because of extra soft-tissue detail (See Table 1).

Real-time MRI interfaces reconstruct and display images geared for interventional procedure guidance (63,64). Multiple concurrent slices can be displayed in 3D to indicate their relative location and orientation (Fig. 5A). Where real-time MRI resolution is inadequate, high-

NIH-PA Author Manuscript

NIH-PA Author Manuscript

NIH-PA Author Manuscript

resolution previous cine or MR angiography roadmaps can also be incorporated to complement the live imaging (Figs. 5B and 5C). Real-time user interfaces (Fig. 6) are now available from commercial system vendors (65). Foot pedals and related remote controls afford the in-room operator some control over scan planes, but interventional MRI usually requires a dedicated scan operator in addition to the interventionist.

When using 2-dimensional imaging techniques, it can be difficult to locate a structure or device that moves out of the selected scan plane. X-ray operators are accustomed to projection views where the entire anatomy or device is visible in the field of view despite its position in the ("through-plane") third dimension. Independent coloring of multiple active device channels and device-only projection views help overcome this problem (63). Alternatively, computer algorithms can locate and even automatically reposition the scan plane to show the entire active MR device in 3 dimensions (66–68). Comparable techniques have been developed to track the position of passive devices (69).

Interventional devices

The same mechanisms that provide unique image contrast during CMR also make most X-ray catheters either invisible or unacceptable for use during iCMR procedures. Metallic cores or braiding that impart catheter pushability and torquability cause imaging artifacts and obscure entire organs. Polymer-only catheters are not visible unless modified and often lack requisite mechanical performance. Conspicuous and safe CMR catheter devices are not generally commercially available but represent an active area of research and development. Interventional CMR devices typically are classified by the mechanism they are visualized in imaging and connection to scanner hardware: passive, semiactive, and active.

Passive devices rely on material properties for visibility during CMR. Material magnetic susceptibility, or how it responds to a magnetic field, can cause inhomogeneities in the main magnetic field that result in signal voids (negative contrast or dark spots) on images. Positive contrast (bright spots) can be generated by the use of paramagnetic T1 shortening contrast agents. Many early passive devices used polymer catheters with ferromagnetic (70) or paramagnetic coatings or rings (71,72). Other approaches include filling catheter balloons with CO_2 (Fig. 7A) (73) or more novel contrast agents such as ^{19}F (74) and hyperpolarized ^{13}C (75) detected with multispectral CMR. Off-resonance imaging techniques (76,77) improve the specificity of the device-related signal but usually sacrifice visibility of surrounding anatomy. Recently, several groups (78,79) have developed sophisticated nonmetallic guidewires that mimic the mechanical properties of metallic X-ray guidewires. They are conspicuous because of small metal (susceptibility) markers. An example of a passive device visualized through magnetic susceptibility effects is shown in Figure 8, where a passive guidewire navigates an iliac artery. Passive devices avoid many of the radiofrequency (RF) safety concerns discussed in the "Ensuring iCMR Safety" section and often are simpler to manufacture. However, they remain difficult to discern from background tissue in vivo, especially within curved vascular structures.

Active devices for interventional CMR incorporate small coils or antennae on independent channels connected to the scanner to track (80) or display the device. "Tracking" requires special CMR pulse sequences to locate the tracking coil in 3D space with the computer-synthesized device position overlaid onto images (Fig. 7B). Active device "imaging" or "profiling" allows a device to be depicted uniquely (for example, based on color) on CMR images acquired in real time. An example is the active guidewire in Figure 7C. Many of the early coil designs for atheroimaging evolved into active catheters and guidewires devices having loop and loopless (81) antenna configurations. It is challenging to incorporate requisite electrical and mechanical components in appropriately sized designs that simultaneously satisfy operators' functional expectations. Clinical-grade active guidewires and catheters are

NIH-PA Author Manuscript

NIH-PA Author Manuscript

NIH-PA Author Manuscript

nearing clinical reality (82), but thorough performance and safety evaluation remains an important step.

Semiactive devices typically contain circuit elements such as inductively coupled markers. These do not require long transmission lines (connecting electrical cables) and need not be connected directly to the scanner but may be more visible than passive devices. Through mutual inductance the signal around the inductively coupled coil can be detected by surface receiver coils. Inductively coupled markers can be incorporated on the end of catheters (83,84), but device visualization is then limited to this segment. Further optical tuning (85,86) or signal separation (87) techniques may be required to clearly distinguish these devices from background imaging.

Ensuring iCMR safety

MRI uses 3 significant electromagnetic fields. The static, permanent magnetic field, B0, can exert tremendous force and torque on ferromagnetic objects, drawing them into the bore. Consequently, instruments, monitoring equipment, and other implements used near MRI scanners must be nonmagnetic or properly labeled and secured to avoid creating dangerous projectiles in the room. Time-varying magnetic field gradients used to create images may cause peripheral nerve stimulation, which limits the slew rate and therefore imaging speed. The vibration of these gradient coils creates the acoustic noise that can be mitigated by the use of hearing protection and MR-compatible communication systems. Finally, the pulsed electromagnetic RF field, B1, used to energize hydrogen spins during imaging, produces a significant heating risk. Long conductors such as cables connecting local receiver coils, electrocardiogram leads, and active CMR devices, when exposed to the changing magnetic fields, can develop induced currents and heat due to resistive losses. More important, coupling with the electrical field component of B1 can store electrical energy along the device that creates heat near the device tips (88). Several approaches have been explored to minimize active device heating, including detuning devices during transmission when RF energy is highest, and the use of RF chokes (89) or transformers (90) in transmission lines to alter their electrical length. Newer optical transmission lines (91) or wireless coils may provide safer alternatives in the future to relay device MR signals to the scanner.

Conclusions: The Future of iCMR

Pre-clinical demonstrations of iCMR have been enticing. The question remains how to bring this technology into the clinic. The requisite imaging capabilities for iCMR are available on commercial MRI systems. Compatible clinical-grade catheter devices remain largely unavailable absent much commercial investment. Academic centers are now independently developing clinical-grade active and passive catheter tools. Although the pace of development has been slow, future opportunities remain rich.

ABBREVIATIONS AND ACRONYMS

3D	3-dimensional
CMR	cardiovascular magnetic resonance
EP	electrophysiology
iCMR	interventional cardiovascular magnetic resonance
RF	radiofrequency
VSD	ventricular septal defect

NIH-PA Author Manuscript

NIH-PA Author Manuscript

NIH-PA Author Manuscript

XFM X-ray–fused with magnetic resonance imaging

References

1. Kantor HL, Briggs RW, Balaban RS. In vivo 31P nuclear magnetic resonance measurements in canine heart using a catheter-coil. Circ Res 1984;55:261–6. [PubMed: 6744535]
2. Hurst GC, Hua J, Duerk JL, Cohen AM. Intravascular (catheter) NMR receiver probe: preliminary design analysis and application to canine iliofemoral imaging. Magn Reson Med 1992;24:343–57. [PubMed: 1569872]
3. Martin AJ, Plewes DB, Henkelman RM. MR imaging of blood vessels with an intravascular coil. J Magn Reson Imaging 1992;2:421–9. [PubMed: 1633395]
4. Nordbeck P, Bauer WR, Fidler F, et al. Feasibility of real-time MRI with a novel carbon catheter for interventional electrophysiology. Circ Arrhythmia Electrophysiol 2009;2:258–67.
5. Raval AN, Telep JD, Guttman MA, et al. Real-time magnetic resonance imaging-guided stenting of aortic co-arctation with commercially available catheter devices in swine. Circulation 2005;112:699–706. [PubMed: 16043639]
6. Omary RA, Green JD, Schirf BE, Li Y, Finn JP, Li D. Real-time magnetic resonance imaging-guided coronary catheterization in swine. Circulation 2003;107:2656–9. [PubMed: 12756160]
7. Serfaty JM, Yang X, Foo TK, Kumar A, Derbyshire A, Atalar E. MRI-guided coronary catheterization and PTCA: a feasibility study on a dog model. Magn Reson Med 2003;49:258–63. [PubMed: 12541245]
8. Spuentrup E, Ruebben A, Schaeffter T, Manning WJ, Gunther RW, Buecker A. Magnetic resonance-guided coronary artery stent placement in a swine model. Circulation 2002;105:874–9. [PubMed: 11854130]
9. Manke C, Nitz WR, Djavidani B, et al. MR imaging-guided stent placement in iliac arterial stenoses: a feasibility study. Radiology 2001;219:527–34. [PubMed: 11323483]
10. Elgort DR, Hillenbrand CM, Zhang S, et al. Image-guided and -monitored renal artery stenting using only MRI. J Magn Reson Imaging 2006;23:619–27. [PubMed: 16555228]
11. Raman VK, Karmarkar PV, Guttman MA, et al. Real-time magnetic resonance-guided endovascular repair of experimental abdominal aortic aneurysm in swine. J Am Coll Cardiol 2005;45:2069–77. [PubMed: 15963411]
12. Eggebrecht H, Kuhl H, Kaiser GM, et al. Feasibility of real-time magnetic resonance-guided stent-graft placement in a swine model of descending aortic dissection. Eur Heart J 2006;27:613–20. [PubMed: 16431874]
13. Krueger JJ, Ewert P, Yilmaz S, et al. Magnetic resonance imaging-guided balloon angioplasty of coarctation of the aorta: a pilot study. Circulation 2006;113:1093–100. [PubMed: 16490822]
14. Raval AN, Karmarkar PV, Guttman MA, et al. Real-time magnetic resonance imaging-guided endovascular recanalization of chronic total arterial occlusion in a swine model. Circulation 2006;113:1101–7. [PubMed: 16490819]
15. Anderson KJ, Leung G, Dick AJ, Wright GA. Forward-looking intra-vascular orthogonal-solenoid coil for imaging and guidance in occlusive arterial disease. Magn Reson Med 2008;60:489–95. [PubMed: 18666117]
16. Kee ST, Ganguly A, Daniel BL, et al. MR-guided transjugular intrahepatic portosystemic shunt creation with use of a hybrid radiography/MR system. J Vasc Interv Radiol 2005;16:227–34. [PubMed: 15713923]
17. Arepally A, Karmarkar PV, Weiss C, Atalar E. Percutaneous MR imaging-guided transvascular access of mesenteric venous system: study in swine model. Radiology 2006;238:113–8. [PubMed: 16373762]
18. Raval AN, Karmarkar PV, Guttman MA, et al. Real-time MRI guided atrial septal puncture and balloon septostomy in swine. Catheter Cardiovasc Interv 2006;67:637–43. [PubMed: 16532499]
19. Elagha AA, Kocaturk O, Guttman MA, et al. Real-time MR imaging-guided laser atrial septal puncture in swine. J Vasc Interv Radiol 2008;19:1347–53. [PubMed: 18725098]

NIH-PA Author Manuscript

NIH-PA Author Manuscript

NIH-PA Author Manuscript

20. Buecker A, Spuentrup E, Grabitz R, et al. Magnetic resonance-guided placement of atrial septal closure device in animal model of patent foramen ovale. Circulation 2002;106:511–5. [PubMed: 12135954]
21. Rickers C, Jerosch-Herold M, Hu X, et al. Magnetic resonance image-guided transcatheter closure of atrial septal defects. Circulation 2003;107:132–8. [PubMed: 12515755]
22. Schalla S, Saeed M, Higgins CB, Weber O, Martin A, Moore P. Balloon sizing and transcatheter closure of acute atrial septal defects guided by magnetic resonance fluoroscopy: assessment and validation in a large animal model. J Magn Reson Imaging 2005;21:204–11. [PubMed: 15723375]
23. Kuehne T, Yilmaz S, Meinus C, et al. Magnetic resonance imaging-guided transcatheter implantation of a prosthetic valve in aortic valve position: feasibility study in swine. J Am Coll Cardiol 2004;44:2247–9. [PubMed: 15582324]
24. McVeigh ER, Guttman MA, Lederman RJ, et al. Real-time interactive MRI-guided cardiac surgery: aortic valve replacement using a direct apical approach. Magn Reson Med 2006;56:958–64. [PubMed: 17036300]
25. Bracken JA, Komljenovic P, Lillaney PV, Fahrig R, Rowlands JA. Closed-bore XMR (CBXMR) systems for aortic valve replacement: X-ray tube imaging performance. Med Phys 2009;36:1086–97. [PubMed: 19472613]
26. Lederman RJ, Guttman MA, Peters DC, et al. Catheter-based endomyocardial injection with real-time magnetic resonance imaging. Circulation 2002;105:1282–4. [PubMed: 11901036]
27. Corti R, Badimon J, Mizsei G, et al. Real time magnetic resonance guided endomyocardial local delivery. Heart 2005;91:348–53. [PubMed: 15710717]
28. Barbash IM, Leor J, Feinberg MS, et al. Interventional magnetic resonance imaging for guiding gene and cell transfer in the heart. Heart 2004;90:87–91. [PubMed: 14676253]
29. Dick AJ, Guttman MA, Raman VK, et al. Magnetic resonance fluoroscopy allows targeted delivery of mesenchymal stem cells to infarct borders in swine. Circulation 2003;108:2899–904. [PubMed: 14656911]
30. Saeed M, Martin A, Jacquier A, et al. Permanent coronary artery occlusion: cardiovascular MR imaging is platform for percutaneous transendocardial delivery and assessment of gene therapy in canine model. Radiology 2008;249:560–71. [PubMed: 18780824]
31. Kraitchman DL, Heldman AW, Atalar E, et al. In vivo magnetic resonance imaging of mesenchymal stem cells in myocardial infarction. Circulation 2003;107:2290–3. [PubMed: 12732608]
32. Andreassi MG, Ait-Ali L, Botto N, Manfredi S, Mottola G, Picano E. Cardiac catheterization and long-term chromosomal damage in children with congenital heart disease. Eur Heart J 2006;27:2703–8. [PubMed: 16717079]
33. Vano E, Gonzalez L, Fernandez JM, Haskal ZJ. Eye lens exposure to radiation in interventional suites: caution is warranted. Radiology 2008;248:945–53. [PubMed: 18632529]
34. Goldstein JA, Balter S, Cowley M, Hodgson J, Klein LW. Occupational hazards of interventional cardiologists: prevalence of orthopedic health problems in contemporary practice. Catheter Cardiovasc Interv 2004;63:407–11. [PubMed: 15558765]
35. Razavi R, Hill DL, Keevil SF, et al. Cardiac catheterisation guided by MRI in children and adults with congenital heart disease. Lancet 2003;362:1877–82. [PubMed: 14667742]
36. Muthurangu V, Taylor A, Andrian-tsimiavona R, et al. Novel method of quantifying pulmonary vascular resistance by use of simultaneous invasive pressure monitoring and phase-contrast magnetic resonance flow. Circulation 2004;110:826–34. [PubMed: 15302793]
37. Kuehne T, Yilmaz S, Schulze-Neick I, et al. Magnetic resonance imaging guided catheterisation for assessment of pulmonary vascular resistance: in vivo validation and clinical application in patients with pulmonary hypertension. Heart 2005;91:1064–9. [PubMed: 16020598]
38. Kuehne T, Saeed M, Higgins CB, et al. Endovascular stents in pulmonary valve and artery in swine: feasibility study of MR imaging-guided deployment and postinterventional assessment. Radiology 2003;226:475–81. [PubMed: 12563142]
39. Khambadkone S, Coats L, Taylor A, et al. Percutaneous pulmonary valve implantation in humans: results in 59 consecutive patients. Circulation 2005;112:1189–97. [PubMed: 16103239]
40. Dickfeld T, Calkins H, Zviman M, et al. Anatomic stereotactic catheter ablation on three-dimensional magnetic resonance images in real time. Circulation 2003;108:2407–13. [PubMed: 14568905]

NIH-PA Author Manuscript

NIH-PA Author Manuscript

NIH-PA Author Manuscript

41. Dickfeld T, Kato R, Zviman M, et al. Characterization of radiofrequency ablation lesions with gadolinium-enhanced cardiovascular magnetic resonance imaging. J Am Coll Cardiol 2006;47:370–8. [PubMed: 16412863]
42. McGann CJ, Kholmovski EG, Oakes RS, et al. New magnetic resonance imaging-based method for defining the extent of left atrial wall injury after the ablation of atrial fibrillation. J Am Coll Cardiol 2008;52:1263–71. [PubMed: 18926331]
43. Susil RC, Yeung CJ, Halperin HR, Lardo AC, Atalar E. Multifunctional interventional devices for MRI: a combined electrophysiology/MRI catheter. Magn Reson Med 2002;47:594–600. [PubMed: 11870847]
44. Dukkipati SR, Mallozzi R, Schmidt EJ, et al. Electroanatomic mapping of the left ventricle in a porcine model of chronic myocardial infarction with magnetic resonance-based catheter tracking. Circulation 2008;118:853–62. [PubMed: 18678773]
45. Krueger S, Lips O, David B, et al. Towards MR-guided EP interventions using an RF-safe concept. J Cardiovasc Magn Reson 2009;11 (Suppl):O84.
46. Nazarian S, Kolandaivelu A, Zviman MM, et al. Feasibility of real-time magnetic resonance imaging for catheter guidance in electrophysiology studies. Circulation 2008;118:223–9. [PubMed: 18574048]
47. Gutierrez LF, Silva R, Ozturk C, et al. Technology preview: X-ray fused with magnetic resonance during invasive cardiovascular procedures. Catheter Cardiovasc Interv 2007;70:773–82. [PubMed: 18022851]
48. de Silva R, Gutierrez LF, Raval AN, McVeigh ER, Ozturk C, Lederman RJ. X-ray fused with magnetic resonance imaging (XFM) to target endomyocardial injections: validation in a swine model of myocardial infarction. Circulation 2006;114:2342–50. [PubMed: 17101858]
49. Ratnayaka K, Raman VK, Faranesh AZ, et al. Antegrade percutaneous closure of membranous ventricular septal defect using X-ray fused with magnetic resonance imaging. J Am Coll Cardiol Intv 2009;2:224–30.
50. Rhode KS, Hill DL, Edwards PJ, et al. Registration and tracking to integrate X-ray and MR images in an XMR facility. IEEE Trans Med Imaging 2003;22:1369–78. [PubMed: 14606671]
51. Rhode KS, Sermesant M, Brogan D, et al. A system for real-time XMR-guided cardiovascular intervention. IEEE Trans Med Imaging 2005;24:1428–40. [PubMed: 16279080]
52. King AP, Boubertakh R, Rhode KS, et al. A subject-specific technique for respiratory motion correction in image-guided cardiac catheterisation procedures. Med Image Anal 2009;13:419–31. [PubMed: 19223220]
53. Tronnier VM, Wirtz CR, Knauth M, et al. Intraoperative diagnostic and interventional magnetic resonance imaging in neurosurgery. Neurosurgery 1997;40:891–902. [PubMed: 9149246]
54. Martin AJ, Larson PS, Ostrem JL, et al. Placement of deep brain stimulator electrodes using real-time high-field interventional magnetic resonance imaging. Magn Reson Med 2005;54:1107–14. [PubMed: 16206144]
55. Weiss CR, Nour SG, Lewin JS. MR-guided biopsy: a review of current techniques and applications. J Magn Reson Imaging 2008;27:311–25. [PubMed: 18219685]
56. Rieke V, Butts Pauly K. MR thermometry. J Magn Reson Imaging 2008;27:376–90. [PubMed: 18219673]
57. Smith KA, Carrino J. MRI-guided interventions of the musculoskeletal system. J Magn Reson Imaging 2008;27:339–46. [PubMed: 18219687]
58. Cleary K, Melzer A, Watson V, Kronreif G, Stoianovici D. Interventional robotic systems: applications and technology state-of-the-art. Minim Invasive Ther Allied Technol 2006;15:101–13. [PubMed: 16754193]
59. Hoult DI, Saunders JK, Sutherland GR, et al. The engineering of an interventional MRI with a movable 1.5 Tesla magnet. J Magn Reson Imaging 2001;13:78–86. [PubMed: 11169807]
60. Griswold MA, Jakob PM, Heidemann RM, et al. Generalized auto-calibrating partially parallel acquisitions (GRAPPA). Magn Reson Med 2002;47:1202–10. [PubMed: 12111967]
61. Kellman P, Epstein FH, McVeigh ER. Adaptive sensitivity encoding incorporating temporal filtering (TSENSE). Magn Reson Med 2001;45:846–52. [PubMed: 11323811]

NIH-PA Author Manuscript

NIH-PA Author Manuscript

NIH-PA Author Manuscript

62. Pruessmann KP, Weiger M, Scheidegger MB, Boesiger P. SENSE: sensitivity encoding for fast MRI. Magn Reson Med 1999;42:952–62. [PubMed: 10542355]
63. Guttman MA, Ozturk C, Raval AN, et al. Interventional cardiovascular procedures guided by real-time MR imaging: an interactive interface using multiple slices, adaptive projection modes and live 3D renderings. J Magn Reson Imaging 2007;26:1429–35. [PubMed: 17968897]
64. Santos JM, Wright GA, Pauly JM. Flexible real-time magnetic resonance imaging framework. Conf Proc IEEE Eng Med Biol Soc 2004;2:1048–51. [PubMed: 17271862]
65. Yutzy SR, Duerk JL. Pulse sequences and system interfaces for interventional and real-time MRI. J Magn Reson Imaging 2008;27:267–75. [PubMed: 18219681]
66. Schirra CO, Weiss S, Krueger S, et al. Toward true 3D visualization of active catheters using compressed sensing. Magn Reson Med 2009;62:341–7. [PubMed: 19526499]
67. George, A.; Derbyshire, J.; Saybasili, H., et al. Fast, robust 3D visualization and automatic slice repositioning ("snap-to") for MR-guided interventions using active device "profiling". Paper presented at: ISMRM 17th Annual Scientific Meeting; April 18 to 24 2009; Honolulu, HI.
68. Elgort DR, Wong EY, Hillenbrand CM, Wacker FK, Lewin JS, Duerk JL. Real-time catheter tracking and adaptive imaging. J Magn Reson Imaging 2003;18:621–6. [PubMed: 14579407]
69. Patil S, Bieri O, Jhooti P, Scheffler K. Automatic slice positioning (ASP) for passive real-time tracking of interventional devices using projection-reconstruction imaging with echo-dephasing (PRIDE). Magn Reson Med 2009;62:935–42. [PubMed: 19585605]
70. Rubin DL, Ratner AV, Young SW. Magnetic susceptibility effects and their application in the development of new ferromagnetic catheters for magnetic resonance imaging. Invest Radiol 1990;25:1325–32. [PubMed: 2279913]
71. Bakker CJ, Hoogeveen RM, Weber J, van Vaals JJ, Viergever MA, Mali WP. Visualization of dedicated catheters using fast scanning techniques with potential for MR-guided vascular interventions. Magn Reson Med 1996;36:816–20. [PubMed: 8946346]
72. Omary RA, Unal O, Koscielski DS, et al. Real-time MR imaging-guided passive catheter tracking with use of gadolinium-filled catheters. J Vasc Interv Radiol 2000;11:1079–85. [PubMed: 10997475]
73. Miquel ME, Hegde S, Muthurangu V, et al. Visualization and tracking of an inflatable balloon catheter using SSFP in a flow phantom and in the heart and great vessels of patients. Magn Reson Med 2004;51:988–95. [PubMed: 15122681]
74. Kozerke S, Hegde S, Schaeffter T, Lamerichs R, Razavi R, Hill DL. Catheter tracking and visualization using 19F nuclear magnetic resonance. Magn Reson Med 2004;52:693–7. [PubMed: 15334594]
75. Magnusson P, Johansson E, Mansson S, et al. Passive catheter tracking during interventional MRI using hyper-polarized 13C. Magn Reson Med 2007;57:1140–7. [PubMed: 17534914]
76. Dharmakumar R, Koktzoglou I, Tang R, Harris KR, Beohar N, Li D. Off-resonance positive contrast imaging of a passive endomyocardial catheter in swine. Phys Med Biol 2008;53:N249–57. [PubMed: 18562781]
77. Edelman RR, Storey P, Dunkle E, et al. Gadolinium-enhanced off-resonance contrast angiography. Magn Reson Med 2007;57:475–84. [PubMed: 17326177]
78. Krueger S, Schmitz S, Weiss S, et al. An MR guidewire based on micro-pultruded fiber-reinforced material. Magn Reson Med 2008;60:1190–6. [PubMed: 18958856]
79. Mekle R, Hofmann E, Scheffler K, Bilecen D. A polymer-based MR-compatible guidewire: a study to explore new prospects for interventional peripheral magnetic resonance angiography (ipMRA). J Magn Reson Imaging 2006;23:145–55. [PubMed: 16374877]
80. Dumoulin CL, Souza SP, Darrow RD. Real-time position monitoring of invasive devices using magnetic resonance. Magn Reson Med 1993;29:411–5. [PubMed: 8450752]
81. Ocali O, Atalar E. Intravascular magnetic resonance imaging using a loop-less catheter antenna. Magn Reson Med 1997;37:112–8. [PubMed: 8978639]
82. Kocaturk O, Kim AH, Saikus CE, et al. Active two-channel 0.035″ guide-wire for interventional cardiovascular MRI. J Magn Reson Imaging 2009;30:461–5. [PubMed: 19629968]
83. Kuehne T, Fahrig R, Butts K. Pair of resonant fiducial markers for localization of endovascular catheters at all catheter orientations. J Magn Reson Imaging 2003;17:620–4. [PubMed: 12720274]

NIH-PA Author Manuscript

NIH-PA Author Manuscript

NIH-PA Author Manuscript

84. Quick HH, Zenge MO, Kuehl H, et al. Interventional magnetic resonance angiography with no strings attached: wireless active catheter visualization. Magn Reson Med 2005;53:446 –55. [PubMed: 15678524]

85. Eggers H, Weiss S, Boernert P, Boesiger P. Image-based tracking of optically detunable parallel resonant circuits. Magn Reson Med 2003;49:1163–74. [PubMed: 12768595]

86. Wong EY, Zhang Q, Duerk JL, Lewin JS, Wendt M. An optical system for wireless detuning of parallel resonant circuits. J Magn Reson Imaging 2000;12:632–8. [PubMed: 11042647]

87. Celik H, Uluturk A, Tali T, Atalar E. A catheter tracking method using reverse polarization for MR-guided interventions. Magn Reson Med 2007;58:1224–31. [PubMed: 18046701]

88. Pictet J, Meuli R, Wicky S, van der Klink JJ. Radiofrequency heating effects around resonant lengths of wire in MRI. Phys Med Biol 2002;47:2973–85. [PubMed: 12222860]

89. Ladd ME, Quick HH. Reduction of resonant RF heating in intravascular catheters using coaxial chokes. Magn Reson Med 2000;43:615–9. [PubMed: 10748440]

90. Weiss S, Vernickel P, Schaeffter T, Schulz V, Gleich B. Transmission line for improved RF safety of interventional devices. Magn Reson Med 2005;54:182–9. [PubMed: 15968655]

91. Fandrey S, Weiss S, Muller J. Development of an active intravascular MR device with an optical transmission system. IEEE Trans Med Imaging 2008;27:1723–7. [PubMed: 19033088]

NIH-PA Author Manuscript
NIH-PA Author Manuscript
NIH-PA Author Manuscript

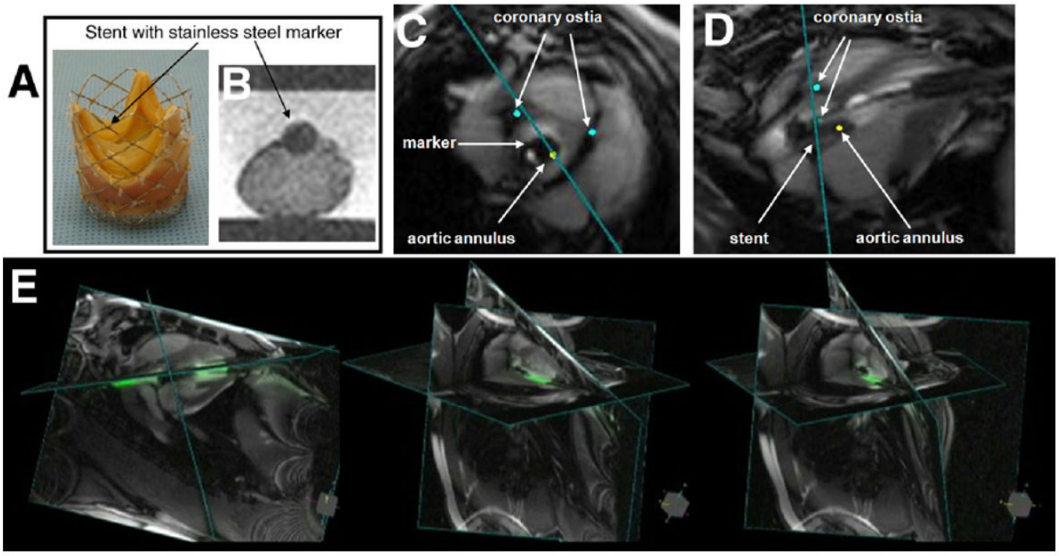

Figure 1. CMR-Guided Transapical Aortic Valve Replacement

(A) Bioprosthesis mounted on a platinum iridium stent with a stainless-steel marker welded on the side of the stent between the commissures. **(B)** The marker is visible as a dark signal in the cardiovascular magnetic resonance (CMR) and indicates the orientation of the prosthesis. Short-axis view and long-axis view of the implanted prosthesis in a pig under real-time CMR are shown in **C** and **D**, respectively. **Blue dots** are digital markers indicating the coronary ostia whereas the **yellow dot** shows aortic annulus location. **(E)** Three-dimensional rendering snapshots show multiple image planes displayed at their relative 3-dimensional position. Images courtesy of Ming Li, PhD, and Keith A. Horvath, MD, Cardiothoracic Surgery Research Program, National Heart, Lung, and Blood Institute.

NIH-PA Author Manuscript

NIH-PA Author Manuscript

NIH-PA Author Manuscript

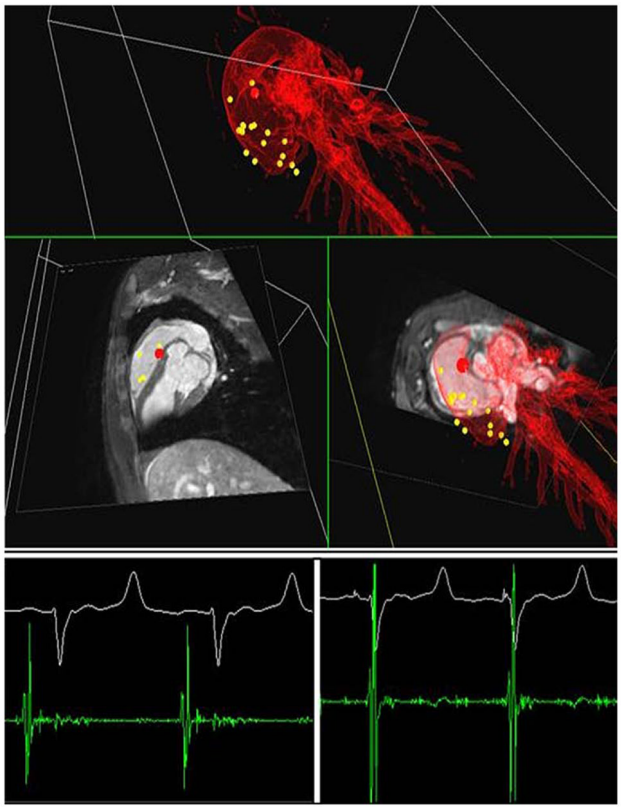

Figure 2. Electrophysiological Cardiac Mapping Under Real-Time CMR Guidance

(Top) Roadmap-based real-time 3-dimensional visualization of the catheter position during recording (**red dot**) on the magnetic resonance-electrophysiological workstation. The **yellow dots** in the 3-dimensional rendering of the heart indicate previous mapping positions. **(Bottom)** In-bore electrophysiological recordings at 2 selected positions showing an atrial signal **(left)** and a ventricular signal **(right)**. Graphic courtesy of Steffen Weiss, PhD, Philips Healthcare.

NIH-PA Author Manuscript
NIH-PA Author Manuscript
NIH-PA Author Manuscript

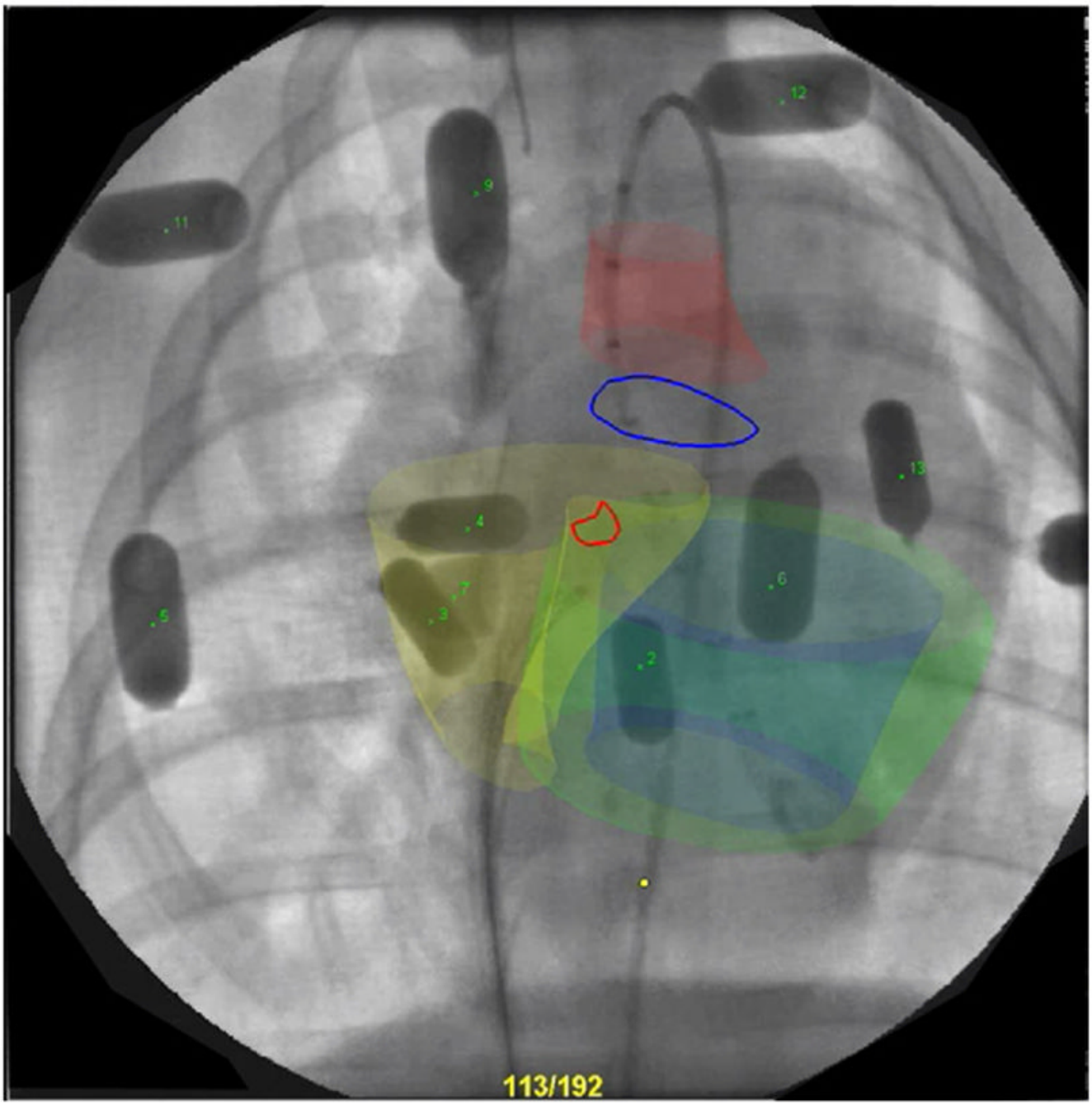

Figure 3. X-Ray Fused With MRI

Representative X-ray fused with magnetic resonance imaging (MRI) display with contours from cardiovascular magnetic resonance (CMR) overlaid on live X-ray. Aorta **(red)**, right ventricle **(yellow)**, left endocardial **(blue)**, and epicardial **(green)** surfaces from CMR shown in 3 dimensions with aortic annulus and ventricular septal defect locations outlined in **blue** and **red**, respectively. Multimodality external fiducial markers also are seen numbered.

NIH-PA Author Manuscript
NIH-PA Author Manuscript
NIH-PA Author Manuscript

Figure 4. Interventional CMR Suite

An interventional cardiovascular magnetic resonance (CMR) suite showing adjacent and interoperable magnetic resonance imaging scanner and X-ray angiography labs. A docking gurney allows rapid intermodality transfer. Courtesy of Alexander J. Dick, MD, Sunnybrook Health Sciences Centre, Toronto.

NIH-PA Author Manuscript

NIH-PA Author Manuscript

NIH-PA Author Manuscript

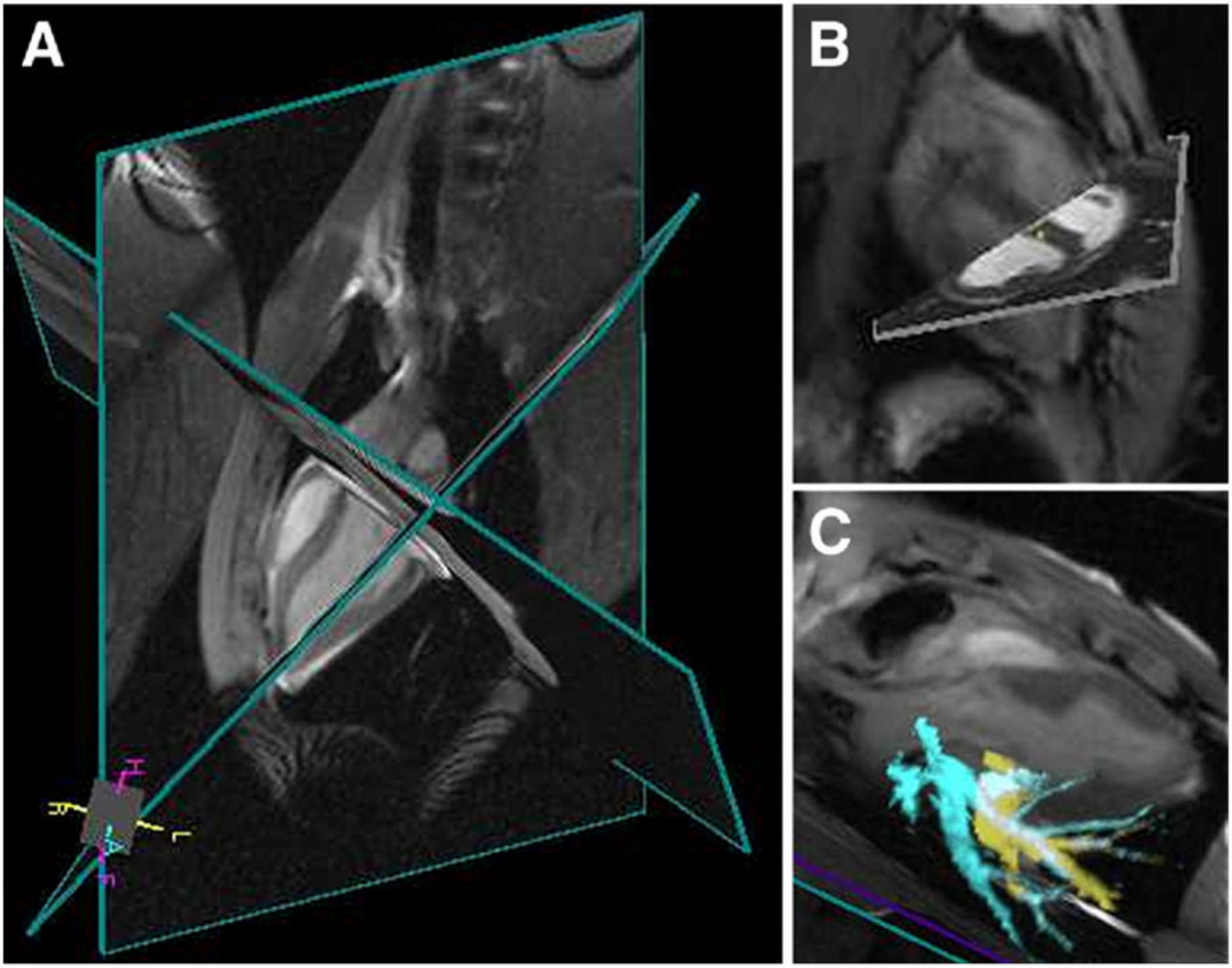

Figure 5. Real-Time Cardiac MR

Multiplanar real-time cardiac imaging at 4 to 5 frames/s **(A)** with pre-acquired static cardiac magnetic resonance (MR) image **(B)** and pulmonary vessel 3-dimensional MR angiography **(C)** roadmaps.

NIH-PA Author Manuscript
NIH-PA Author Manuscript
NIH-PA Author Manuscript

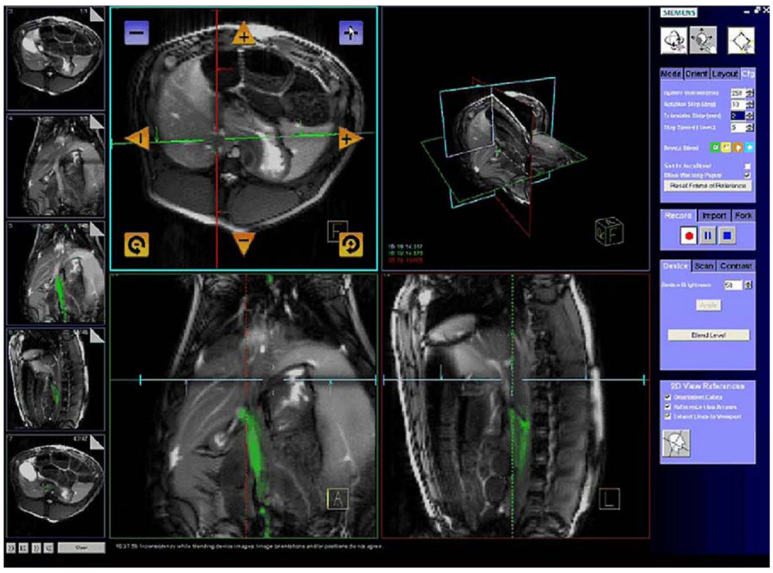

Figure 6. Real-Time MRI User Interface Showing MR-Guided Delivery and Biopsy of Encapsulated Human Islet Cells in a Pig

Example of a real-time magnetic resonance imaging (MRI) user interface from Siemens. Similar interfaces are available for Philips and GE systems. Features include scan plane manipulation, independent device channel coloring, 3-dimensional viewing window, static image roadmaps, and quick access to select slice orientations. Figure courtesy of Christine H. Lorenz, PhD, Siemens Corporate Research, Inc., and Aravind Arepally, MD, Johns Hopkins Medical Institutions, Baltimore, Maryland.

NIH-PA Author Manuscript

NIH-PA Author Manuscript

NIH-PA Author Manuscript

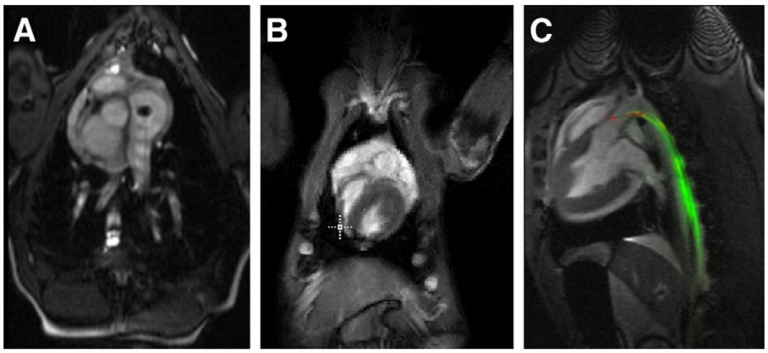

Figure 7. Interventional CMR Devices

Three representative approaches to catheters designed to be tracked using cardiovascular magnetic resonance (CMR). **(A)** Passive nonbraided balloon catheter filled with CO_2 in a right atrium. **(B)** Active tracking catheter in the right heart. Image courtesy of Michael Bock, PhD, German Cancer Research Center (DKFZ), Heidelberg, Germany. **(C)** Two-channel active guidewire in the aorta approaching the left heart.

NIH-PA Author Manuscript
NIH-PA Author Manuscript
NIH-PA Author Manuscript

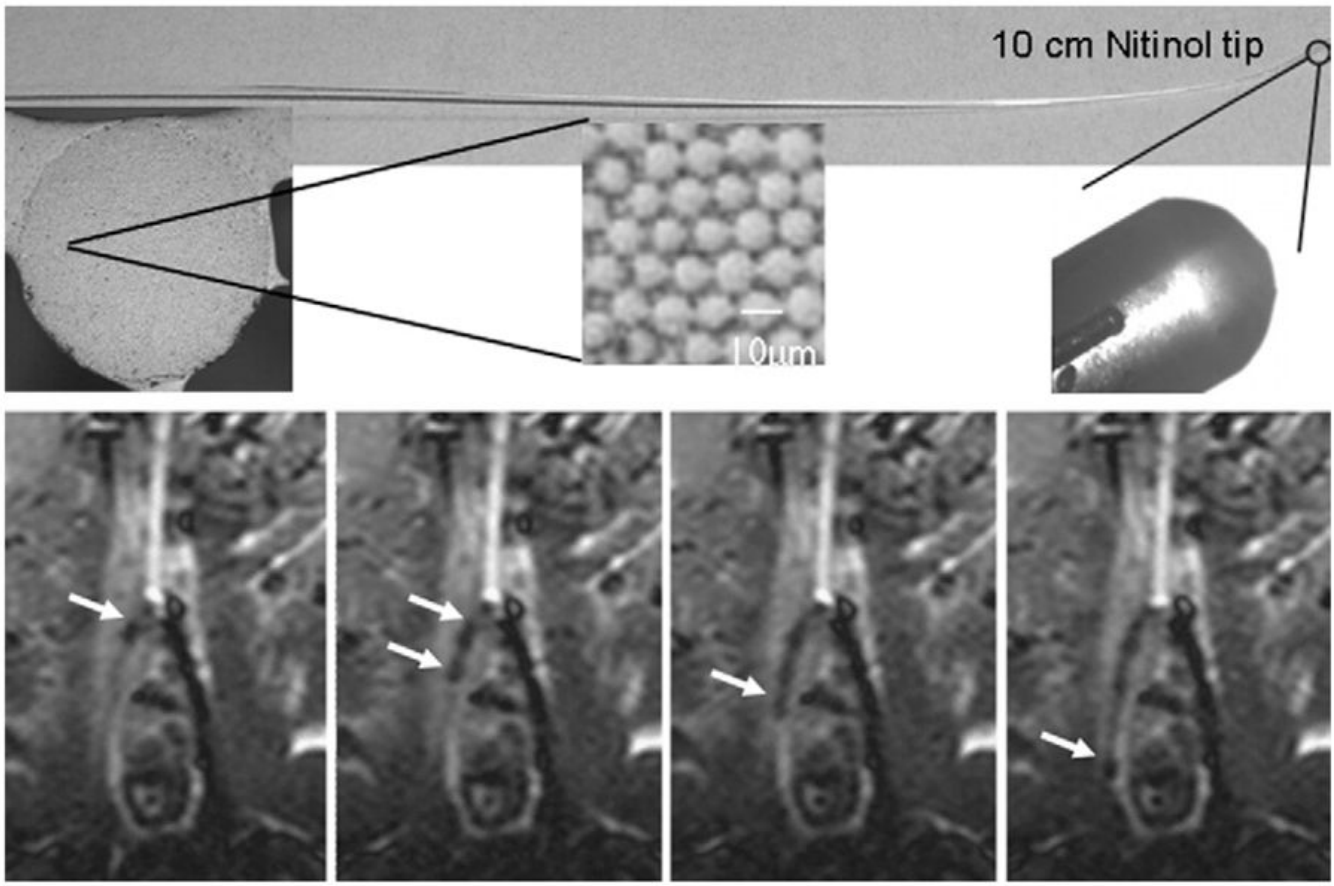

Figure 8. Iliac Artery Navigation Using a Passive Guidewire

(Top) Polymer guidewire with a Nitinol tip. **(Bottom)** Magnetic resonance-guided probing of the contralateral iliac artery with the guide-wire **(arrows)** and a catheter. Susceptibility artifacts in cardiovascular magnetic resonance (CMR) images arise from the iron doped guide-wire, which is also visible under fluoroscopy. These artifacts partially obscure the target tissue. Images courtesy of Gabriele A. Krombach, MD, Department of Diagnostic Radiology, University Hospital Aachen, Aachen, Germany.

NIH-PA Author Manuscript

NIH-PA Author Manuscript

NIH-PA Author Manuscript

Table 1

Comparison of Imaging Modalities for Real-Time Procedural Guidance

	Real-Time CMR	X-Ray	Echocardiography (Surface or Intracavitary)	Computed Tomography
Ionizing radiation	No	Yes	No	Yes
Structures depicted	Hydrogen (or other magnetic nuclei) containing-tissues	X-ray attenuating (iodinated contrast-filled structures, bone)	Echo dense and echo reflective	Bone and soft tissue
Typical spatial resolution	1.5 × 2 × 5 mm*	<0.4 mm	0.6–1 mm	1–2 mm isotropic
Typical frame rate	5–10 frames/s*	15–30 frames/s	20–30 frames/s	2–4 frames/s
Advantages	No ionizing radiation	Widely deployed	Portable	Multislice
	Multiplanar views	Numerous devices available	Lower cost	
	Soft-tissue contrast	High temporal and spatial resolution	High SNR	
	Novel contrast mechanisms		Flow and motion measurements	
Disadvantages	High magnetic field limits devices	Radiation exposure	Limited acoustic windows	Excessive radiation doses
	Low SNR	Limited soft tissue discrimination	Air and device shadowing	Iodinated contrast
	Potential RF heating	Projection-only (2D) views	Limited “context” (field of view)	
	Gadolinium contrast	Iodinated radiocontrast		

*Note the frame rate and spatial resolution given for CMR are arbitrary and represent a typical compromise between spatial and temporal resolution at 1.5-T using parallel imaging with an acceleration factor of 2.

CMR = cardiovascular magnetic resonance; RF = radiofrequency; SNR = signal-to-noise ratio.